Advances in
Geo-Energy Research

Vol. 11, No. 2, p. 141-151, 2024

Original article

# Mechanism of shale oil displacement by $CO_2$ in nanopores: A molecular dynamics simulation study

Zhengbin Wu[1,2], Zhe Sun [2], Kun Shu[3], Shu Jiang[1]*, Qiyang Gou[1], Zhangxing Chen[2]

[1] *Key Laboratory of Theory and Technology of Petroleum Exploration and Development in Hubei Province, China University of Geosciences, Wuhan 430074, P. R. China*

[2] *Department of Chemical and Petroleum Engineering, University of Calgary, Calgary T2N 1N4, Alberta, Canada*

[3] *Research Institute of Exploration & Development, PetroChina Tuha Oilfield Company, Hami 839009, P. R. China*

**Keywords:**
Shale oil
molecular dynamics simulation
micro mechanisms
enhanced oil recovery

**Cited as:**
Wu, Z., Sun, Z., Shu, K., Jiang, S., Gou, Q., Chen, Z. Mechanism of shale oil displacement by $CO_2$ in nanopores: A molecular dynamics simulation study. Advances in Geo-Energy Research, 2024, 11(2): 141-151.
https://doi.org/10.46690/ager.2024.02.06

**Abstract:**
Utilizing $CO_2$ to enhance shale oil recovery has a huge potential and thus has gained widespread popularity in recent years. However, the microscopic mechanisms of $CO_2$ enhancing shale oil recovery remain poorly understood. In this paper, the molecular dynamics simulation method is adopted to investigate the replacement behavior of $CO_2$ in shale oil reservoirs from a micro perspective. Three kinds of *n*-alkanes are selected as the simulative crude oil in silica nanopores. Molecular dynamics models are established to study the occurrence patterns of different alkanes on the rock surface and the alkane-stripping characteristics of $CO_2$. The fluid density, mean square displacement and centroid variation are evaluated to reveal the effect of $CO_2$ on alkanes. The results indicate that different alkanes exhibit varying occurrence characteristics of oil film on the rock surface of the shale reservoir. Specifically, a higher carbon number leads to a thicker oil film. Through the alkane molecular gaps, $CO_2$ penetrates the alkane molecular system and reaches the rock surface to effectively strip the oil film of different alkane molecules. $CO_2$ will more readily mix with the stripped oil molecules and displace them from the rock surface when the carbon number is small. The process for $CO_2$ replacing crude oil on the rock surface can be divided into four typical stages, namely, $CO_2$ diffusion, competitive adsorption, emulsification and dissolution, and $CO_2$-alkanes miscible phase (for light alkanes). This study contributes to the improvement of micro-scale enhanced oil recovery mechanisms for shale oil via $CO_2$ injection and provides a guidance for enhancing shale oil recovery by using $CO_2$.

## 1. Introduction

With the increasing global energy demand, oil and gas production is shifting from conventional to unconventional. The shale oil and gas revolution, which originated in the United States and Canada, is transforming the world's oil and gas supply pattern. Shale reservoirs as unconventional energy sources are characterized by low permeability and porosity due to the extensive development of nanoscale pores (Gou et al., 2019; Dong et al., 2023a). Under the conventional development conditions of horizontal fracturing, the movable reserves of shale oil are generally less than 10%, along with problems such as poor oil recovery effect, rapid production decline and low reservoir recovery efficiency. Field tests and applications have demonstrated that $CO_2$ can effectively exploit oil and gas resources in shale reservoirs and achieve superior production enhancement (Michael et al., 2013; Sheng, 2017; Alafnan, 2022; Wan et al., 2024). Under the formation condition, $CO_2$ is in a supercritical state and has a special property that its density is close to that of liquid and its viscosity is close to that of gas. $CO_2$ is highly diffusible and can enter pores larger than its molecular diameter (0.33 nm). With the multiple actions of energy enhancement, viscosity reduction and phase miscibility, the remaining oil in deep nanoscale pores of shale reservoir can be used effectively, which is a

---

*Corresponding author.

*E-mail address*: wuzb@cug.edu.cn (Z. Wu); zhe.sun@ucalgary.ca (Z. Sun); shukunyjy@petrochina.com.cn (K. Shu); jingsu@cug.edu.cn (S. Jiang); gouqiyang1003@163.com (Q. Gou); zhachen@ucalgary.ca (Z. Chen).

Yandy Scientific Press

Received October 14, 2023; revised December 5, 2023; accepted December 28, 2023; available online January 3, 2024.

realistic avenue for enhancing shale oil recovery. After $CO_2$ injection into the formation, the effects between $CO_2$ and crude oil mainly include the formation of the miscible phase of $CO_2$ and crude oil, the stripping of adsorbed crude oil on the rock surface, and the displacement of oil phase in the rock pores. Due to the difficulty of obtaining deep core samples, the harsh experimental conditions at the nanoscale, and the nano-confined conditions, the traditional petroleum geology theory and flow theory may not be suitable for oil and gas research in nanopores; therefore, the importance of simulation technology has become increasingly prominent (Feng et al., 2020; Jin and Firoozabadi, 2022).

In recent years, molecular dynamics (MD) simulation technology has become an important research method in the field of shale oil development (Pathak et al., 2018; Cui et al., 2022; Sun et al., 2023). This technique can not only make up for the shortcomings of experimental nanoscale research and reduce the relevant costs but also reveal the dynamic behavior of shale oil in confined space and the microscopic interaction mechanism with the rock wall based on atomic details. Therefore, research on the development of shale oil using $CO_2$ based on MD simulations is helpful to clarify the mechanisms of $CO_2$ enhanced oil recovery (EOR) at the nanoscale and enrich the relevant theories of $CO_2$ development of shale oil. Wang et al. (2015, 2016b, 2021) performed MD simulation runs to study the occurrence state of liquid alkanes in organic-rich shale pores and revealed the periodic fluctuations of the density distribution of alkanes. They found that near a solid wall, alkanes form a "solid-like layer" with a density 1.5∼3 times that of a free fluid, and the predominant form of adsorption is multilayer. The number of adsorption layers is affected by fracture width and fluid composition, and the thickness of each adsorption layer is consistent with the width of an alkane molecule. Meanwhile, the adsorption capacity of heavy components on an organic matter surface is stronger. Based on the thickness and average density of each adsorption layer obtained by MD simulation, and considering the different occurrence states of crude oil in a reservoir, the researchers separated the adsorption state and the free state of crude oil and established a petrophysical model and a mathematical model for shale oil resource estimation. Furthermore, they explored the microscopic flow law of shale oil in pore throats of typical shale minerals such as quartz, organic matter and calcite. The results indicated that the flow characteristics of crude oil in nanopores composed of different rocks and minerals are markedly different. Under the same conditions, oil flow is fastest in organic pores, followed by quartz pores, and it is slowest in calcite pores. It was revealed that the physical mechanism of this phenomenon is related to a fluid-solid interaction force and a surface friction coefficient. Santos et al. (2018) used MD simulation to study the behavior of $CO_2$ and *n*-alkanes confined in calcite nanopores. Their results showed that $CO_2$ can effectively displace the alkanes adsorbed on a calcite surface, and that the amount of calcium ions determines the $CO_2$ adsorbed on the pore surface. In addition, the $CO_2$ content, pore size, temperature, and the length of *n*-alkanes are the key parameters that affect the competitive adsorption of $CO_2$ and alkanes on calcite surfaces. Jin et al. (2017) carried out a series of experiments for the comprehensive characterization of rock fluid and $CO_2$ extraction using samples from the Bakken shale. High-pressure mercury tests revealed that the Bakken shale has an average pore throat radius of 3.5 nm, creating high capillary pressures in these pores that increase the difficulty of fluid flow through the rock. Under reservoir conditions, $CO_2$ could extract 15%∼65% of the hydrocarbons from 11 mm diameter Bakken shale samples within 24 hours. Fang et al. (2019) comprehensively discussed the mechanisms of $CO_2$ extraction of hydrocarbons from shale oil reservoirs through MD simulations. Their results showed that the inlet effect caused by a decrease in the adsorption amount of $CO_2$ and the inhibition of continuous oil extraction due to the destruction of dissolution gradient are two key factors driving the extraction process. Yan et al. (2017) used MD simulation to study the dynamic process of oil droplets passing through nanopore throats in a water-containing environment. They found that the oil droplets need to overcome great resistance when passing through the nanopore throats, which is caused by the deformation of oil droplets, an interaction between oil and pores, and the Jamin effect. In addition, they explored the promoting effect of $CO_2$ on the transport process of oil droplets in nanopore throats and analyzed the activation mechanism of $CO_2$ from three aspects: expansion of oil droplets, interaction between oil and pores, and change in the interfacial tension at an oil-water interface.

The density of supercritical $CO_2$ ($scCO_2$) is close to that of a liquid, and it has extremely high solubility in organic solutes. At the same time, the viscosity of $scCO_2$ is low and its diffusion coefficient is about 100 times that of a liquid, so it has high mass transfer capacity. The diffusion of $scCO_2$ into the oil phase can expand the crude oil, reducing its viscosity and improving its mobility. $CO_2$ can easily reach the supercritical state of critical temperature 34.1 °C and critical pressure 7.38 MPa, which reduces the difficulty of $CO_2$ flooding construction (Alfarge et al., 2017). Liu et al. (2017) studied the adsorption and migration behavior of $scCO_2$ and dodecane in inorganic shale nanopores under $scCO_2$ injection at different rates through non-equilibrium molecular dynamics simulation. Hydrogen bonds easily form between $scCO_2$ and hydroxyl groups, and $scCO_2$ preferentially organizes into layered structures on the pore surface after injection. Due to the competitive adsorption between $scCO_2$ and dodecane, the dodecane originally adsorbed on the pore surface is stripped off, leaving more fluid oil in the pores and increasing oil production. Meanwhile, a miscible zone formed between $scCO_2$ and dodecane plays an important role in the displacement process. Wang et al. (2016a) simulated the static properties and flow behaviors of octane and $scCO_2$ confined in slit carbonaceous organic nanopores. Their results indicated that $scCO_2$ is preferentially adsorbed on matrix surfaces over octane and methane, and that the velocity distribution in the slits is piston-like under a pressure gradient, which is significantly different from a parabolic profile in inorganic nanopores. Xue et al. (2022) studied the process of $scCO_2$ dissolution in kerogen on $SiO_2$ surfaces and the flow rate of decane under gas flooding via MD simulation. It was found that $scCO_2$ can effectively dissolve in kerogen adsorbed on

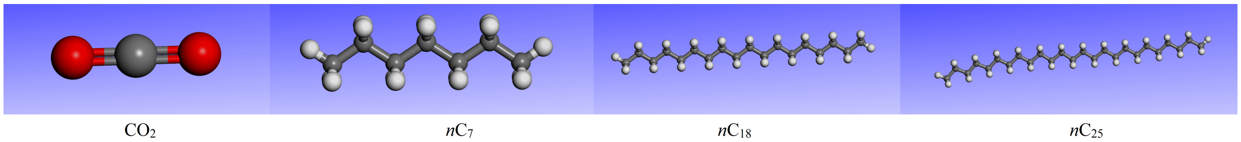

**Fig. 1**. The molecular structures of different materials used in the simulation.

shale surfaces, and the interaction between kerogen and shale surfaces after dissolution is greatly reduced; thus, kerogen can be easily extracted from oil shale. The dissolution capacity of $scCO_2$ increases effectively with increasing pressure up to a critical value (about 50 MPa).

In general, the effect of $CO_2$ in a reservoir environment is the overall result of the interaction of various systems. For reservoirs characterized by a complex environment, to further improve the recovery of crude oil, it is necessary to clarify the basic principle of oil and gas interaction at the microscale. Breakthroughs in the traditional reservoir theoretical analysis methods and the exploration of new means suitable for the microscopic mechanisms of $CO_2$-EOR in shale/tight reservoirs are the promising directions for theoretical research at micro/nano-scale. To this end, the improvement of MD simulation is expected to make great contributions. In addition, clarifying the action law of $CO_2$ with shale oil at the confined nanospace and the elaboration of relevant theories and simulation methods of $CO_2$-EOR for shale oil can provide basic theoretical support for rapid breakthroughs in shale oil development technology. Thus far, most scholars have chosen one kind of alkane as the simulated oil to study the flow of shale oil and the displacement characteristics of $CO_2$ in nanopores, while comparisons between different components in actual shale oils are lacking. Furthermore, the visualized interaction mechanisms between $CO_2$ and alkanes in molecular perspective need to be investigated. This paper focuses on elucidating the micro-replacement mechanisms of $scCO_2$ for shale oil in nanopores; *n*-alkanes, including $nC_7$, $nC_{18}$ and $nC_{25}$, are selected as the crude oil and simulated using the MD method. The results intuitively present the stripping process of $CO_2$ for alkane molecules from the rock surface, providing a theoretical basis for the application of $CO_2$ for shale oil recovery.

## 2. Molecular dynamics simulation method

$CO_2$ is selected to simulate the MD processes of injected gas at the nano-scale in a shale reservoir. The COMPASS II force field has significant advantages in studying the interaction between organic and inorganic molecules and can fully cover the temperature and pressure conditions of the reservoir due to its wide range of temperature and pressure adaptation (Guo et al., 2022). Therefore, this study is carried out by Materials Studio (MS) software (version 2020) and the COMPASS II force field is used as the foundation of a MD force field system. Hydrophilic $SiO_2$ is taken as the basic mineral molecule to construct an $\alpha$-$SiO_2$ surface and simulate a rock wall. To compare the interactions between different alkanes and $CO_2$, three kinds of *n*-alkanes ($nC_7$, $nC_{18}$, and $nC_{25}$) are set as the simulated crude oil. Considering that resins and asphaltenes are also important components of crude oil, $nC_{25}$ can be used to compare the occurrence and replacement characteristics between light and heavy components. The specific molecular configurations are shown in Fig. 1.

### 2.1 Rock system

The intrinsic $\alpha$-$SiO_2$ in MS is selected as the basis to construct a certain thickness of quartz surface. In a reservoir environment, under the influence of natural mineral water, a rock wall will be charged. Therefore, hydrogenation is carried out on the $\alpha$-$SiO_2$ surface to construct a hydroxylated rock surface. The adsorption effect of Coulomb force is added to the interaction with crude oil or injected molecules.

### 2.2 Oil system

A certain number of *n*-alkane molecules (the specific number depends on lattice volume and density) are constructed on the surface of $\alpha$-$SiO_2$, and the oil film molecules are kept in contact with the rock wall. Then, dynamic simulation is carried out for 0.2 ns. Finally, the alkanes with stable distributions on the surface of $\alpha$-$SiO_2$ are obtained (i.e., the occurrence characteristics of crude oil).

### 2.3 Basic parameters

In the construction of different alkane-$\alpha$-$SiO_2$ systems, the main simulation parameters include the size of the system, the number of alkanes and the system environment. Due to the varying properties of alkanes, the density and number of molecules are different when a system is constructed with the same volume. In this paper, the temperature of the system is set as 323.15 K, and NVT ensemble is selected as the basic system setting. The pressure conditions are set by the system density. The densities of $nC_7$, $nC_{18}$, and $nC_{25}$, and $CO_2$ in the nanospace are 0.63, 0.78, 0.88, and 0.78 g/cm$^3$, respectively. The molecular numbers of $nC_7$, $nC_{18}$, and $nC_{25}$, and $CO_2$ are 270, 135, 108, and 2,600, respectively. The size of $\alpha$-$SiO_2$ rock surface is $59.4\times58.9\times12.6$ Å. During the process of $CO_2$ replacing oil, to eliminate the effect of the periodic boundary in the z direction of the system, an extra vacuum layer of 29.6 Å is set on the top layer, so that a stable initial $CO_2$-oil-rock system is constructed. Below the vacuum layer, a $CO_2$ layer of 5.2 Å with a high density of 1.5 g/cm$^3$ is set to prevent $CO_2$ from escaping.

After the establishment of the basic model, 10 ps dynamic simulations of the system are carried out to ensure energy stability. Then, MD simulations are performed for 0.2 ns with a step size of 1.0 fs. The track and dynamic recording steps are 200. The density cannot be directly calculated in MS but can be obtained by relative concentration distribution provided

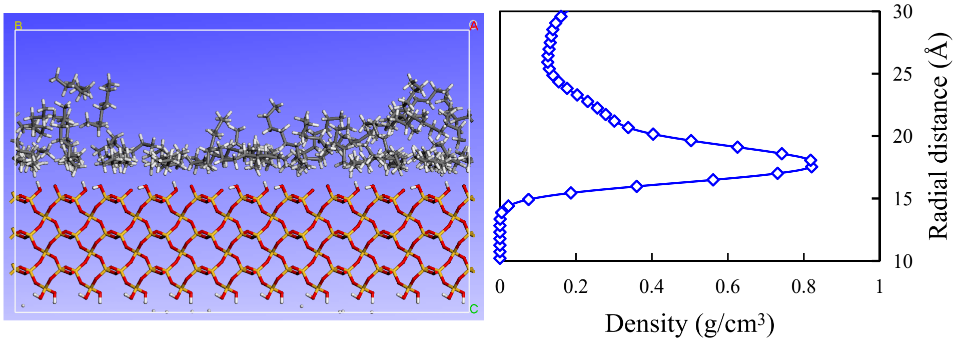

(a) $nC_7$

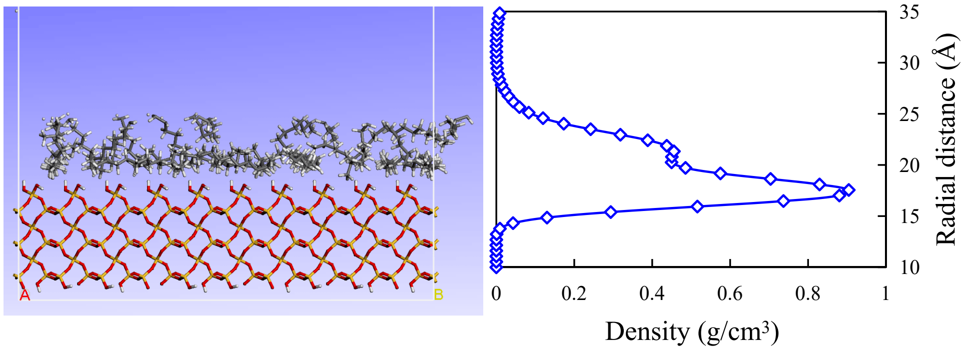

(b) $nC_{18}$

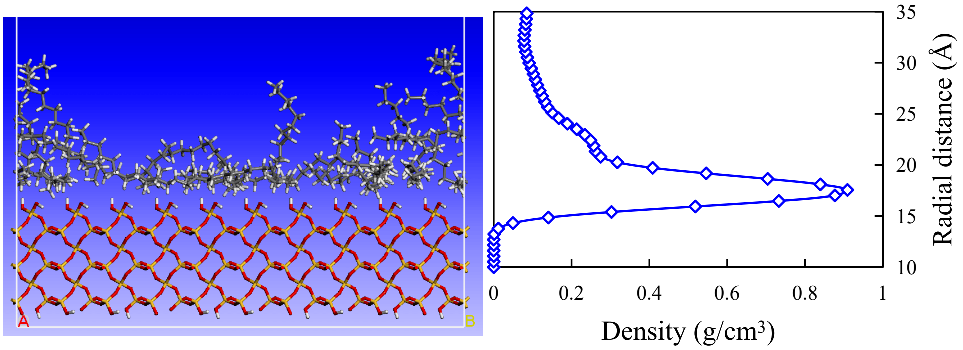

(c) $nC_{25}$

**Fig. 2**. Occurrence state (left) and vertical density distribution characteristics (right) of alkanes on the surface of $\alpha$-$SiO_2$.

by the Concentration Profile function in the Forcite module of MS. The calculation principle is briefly explained below.

The definition of dimensionless concentration ($C_r$) in a coordinate direction in a system is:

$$C_r = \frac{C_s}{C_b} \tag{1}$$

where $C_s$ and $C_b$ refer to the number densities of a component in a small slab and a box (bulk), respectively; namely, the concentrations are:

$$C_s = \frac{n_s}{V_s} \tag{2}$$

$$C_b = \frac{n_b}{V_b} \tag{3}$$

where $n$ represents the number of molecules; $V$ is the volume of a certain unit.

The density along a coordinate direction ($\rho_s$) can be converted with the use of bulk density ($\rho_b$) as follows:

$$\rho_s = C_r \times \rho_b \tag{4}$$

## 3. Results and discussion

### 3.1 Occurrence characteristics of different alkanes on the $\alpha$-$SiO_2$ surface

After 0.2 ns of MD simulation, the occurrence characteristics of alkanes ($nC_7$, $nC_{18}$, and $nC_{25}$) on the surface of $\alpha$-$SiO_2$ are shown in Fig. 2. The vertical distribution of oil molecule density is selected to compare the distribution characteristics of different alkane molecules on the surface of $\alpha$-$SiO_2$.

Different from the multi-layer oil film of octane ($C_8$) adsorbed on silica silt (Wang et al., 2016b), $nC_7$, $nC_{18}$, and

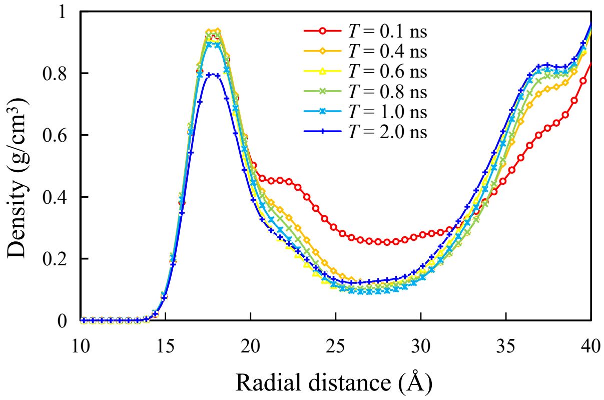

**Fig. 3**. Radial density changes of $nC_7$ on $\alpha$-$SiO_2$ surface.

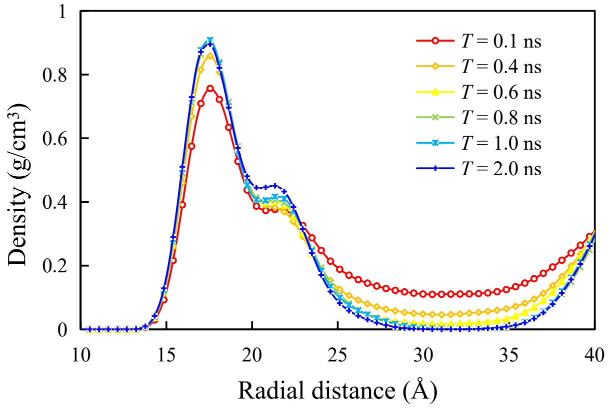

**Fig. 4**. Radial density changes of $nC_{18}$ on $\alpha$-$SiO_2$ surface.

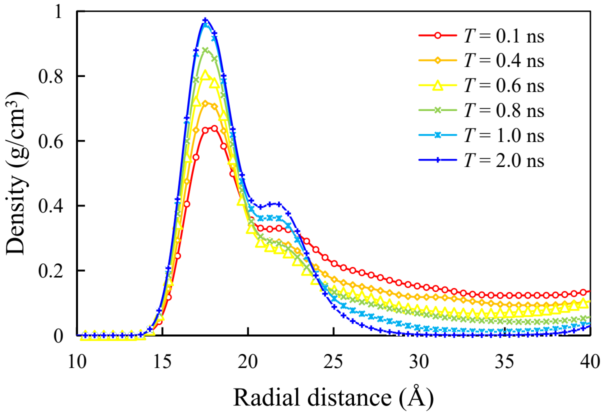

**Fig. 5**. Radial density changes of $nC_{25}$ on $\alpha$-$SiO_2$ surface.

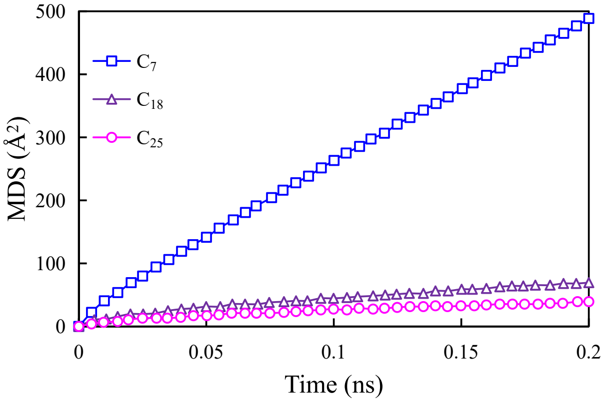

**Fig. 6**. Comparison of MSD of different alkane molecules.

$nC_{25}$ present the occurrence characteristics of single oil film. Fig. 2(a) depicts the occurrence state of $nC_7$ after 0.2 ns of dynamic simulation; there is an obvious peak at 17.5 Å from the outermost layer to the surface of $\alpha$-$SiO_2$, reaching 0.82 g/cm$^3$, which indicates that $nC_7$ molecules exist in the inner layer of $\alpha$-$SiO_2$ in the form of an oil film that is characterized by a single molecular layer, while the alkane molecules of the outer layer cannot form a dense and continuous oil film distribution state. This is because the $nC_7$ molecules themselves are relatively active and have strong free movement ability. While being affected by a rock surface, they can still exhibit violent movement under the influence of the outer boundary (Huang et al., 2024). The occurrence states of $nC_{18}$ molecules on the surface of $\alpha$-$SiO_2$ (Fig. 2(b)) show that as the carbon number of alkane increases, the thickness of the oil film does not continue to rise. The oil film density reaches 0.95 g/cm$^3$ at 16.4 Å from the $\alpha$-$SiO_2$ surface. After the formation of a strongly adsorbed oil film, it significantly weakens the attraction effect of $SiO_2$ on the alkanes in the outer layer. At the same time, $nC_{18}$ has a higher molecular weight, which requires a stronger force to affect the motion state of $nC_{18}$. As a result, the $nC_{18}$ molecules present the state of a thin and single-layer oil film. The occurrence states of alkane molecules on the surface of $\alpha$-$SiO_2$ show that the oil film increases from $nC_7$ to $nC_{18}$, while the increase in oil film thickness from $nC_{18}$ to $nC_{25}$ is not significant. From the vertical density distribution of $nC_{25}$ in Fig. 2(c), it can be determined that the density of $nC_{25}$ is 0.98 g/cm$^3$ at the distance of 17.3 Å. However, due to the large molecular size of $nC_{25}$, the density distribution does not become narrower.

In order to clarify the process of forming such an occurrence state of alkanes, the dynamic curves of radial density changes (Figs. 3-5) and the mean square displacement (MSD) curves (Fig. 6) of different alkanes molecules were compared. It can be seen from Fig. 3 that for $nC_7$ molecules with a smaller molecular weight, it is easy to form a thin oil film layer; they are rapidly adsorbed on the surface of $\alpha$-$SiO_2$. Subsequently, they gradually migrate inwards with further adsorption on the $\alpha$-$SiO_2$ surface. For $nC_{18}$ and $nC_{25}$ with higher molecular weights, the formation of a stable oil film is significantly different from that for $nC_7$. As can be seen from Fig. 4, when $nC_{18}$ molecules contact the $\alpha$-$SiO_2$ surface, the characteristics of the oil film also appear immediately; however, the density of the initial oil film is relatively small. With an increase in the alkane molecular weight, the occurrence characteristics of the oil film presented by $nC_{25}$ are similar to those for $nC_{18}$ (Fig. 5), but the formation time of a stable oil film is obviously different.

Based on the molecular motion processes on the surface of alkane-$\alpha$-$SiO_2$, it can be found that alkanes with both large and small molecular weight show the characteristics of an oil film. Specifically, $nC_7$ with a lower carbon number and other alkanes with a carbon number $> 18$ are single-layer oil films, which results from an insufficient acting force. In addition,

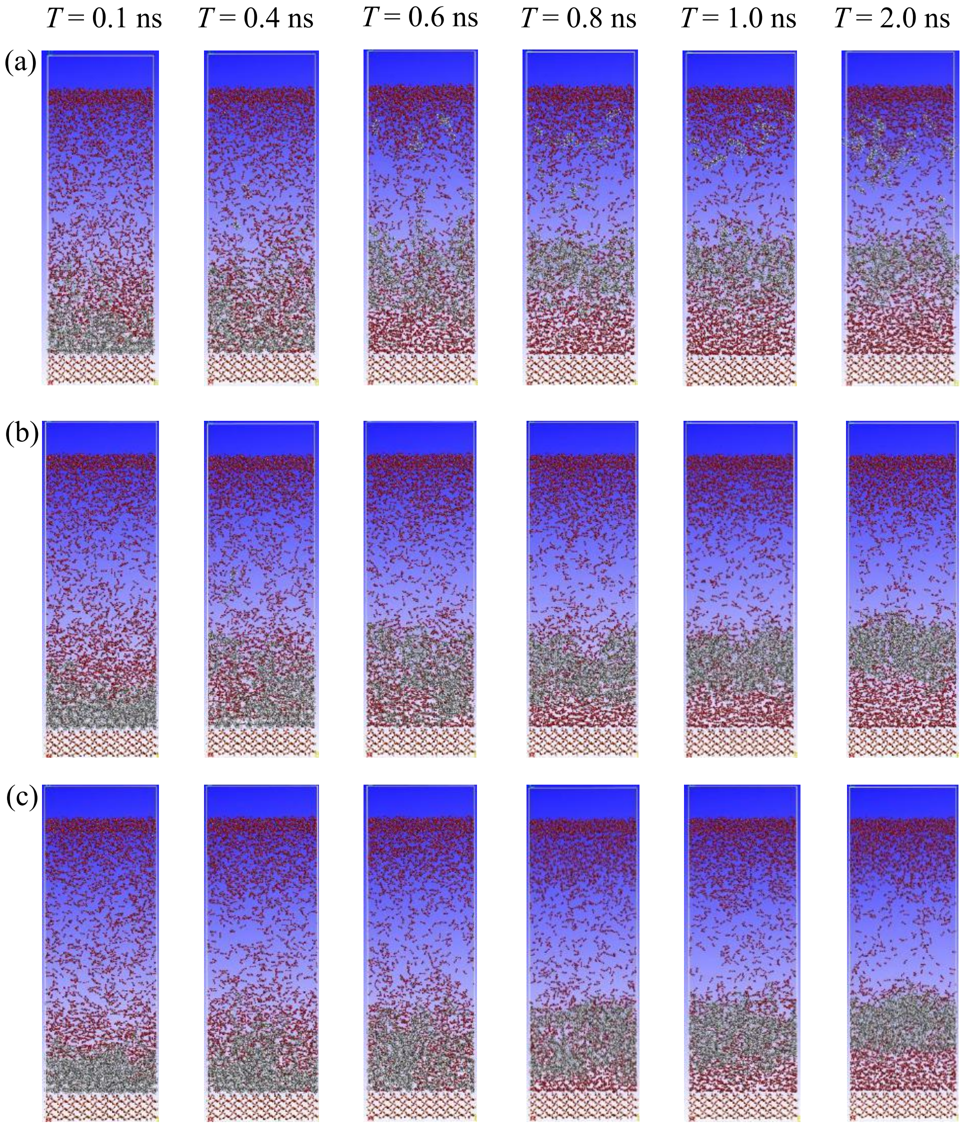

**Fig. 7**. MD simulation for the stripping characteristics of $CO_2$ for oil on $\alpha$-$SiO_2$ surface, (a) $n C_7$, (b) $n C_{18}$, and (c) $n C_{25}$.

alkanes with larger molecular weight usually have a longer molecular chain. Alkanes in the innermost position near the surface of $\alpha$-$SiO_2$ suffice to present a flat oil film state. The molecules in the outer layer do not contact with the $\alpha$-$SiO_2$ surface directly, and they are difficult to spread as an oil film. From the MSD of different alkanes in Fig. 6, it can be found that the free motion ability of $n C_7$ alkanes is the strongest. For alkanes with large molecular weight above $n C_{18}$, the free motion ability decreases rapidly.

### 3.2 Replacement characteristics of $CO_2$ for oil on $\alpha$-$SiO_2$ surface

From the molecular motion trajectories of $CO_2$-alkanes-$\alpha$-$SiO_2$ surface systems in Fig. 7, it can be established that the replacement effect of $CO_2$ for light alkanes is obviously better than that for heavy alkanes. Meanwhile, the dispersion states of light alkanes and heavy alkanes after replacement are also very different.

As illustrated in Fig. 7(a), $CO_2$ can rapidly move towards the rock wall through intermolecular gaps between $n C_7$ molecules. At about 0.4 ns, a considerable number of $CO_2$ molecules have already been adsorbed on the rock surface. At the same time, the system is fully stretched when it is mixed with $CO_2$ and the dispersion becomes stronger. The free movement ability of $n C_7$ molecules is also strengthened. At 0.8 ns, $CO_2$ completely strips $n C_7$ molecules from the rock surface, and then it is further mixed fully with $n C_7$ until the system becomes homogeneous. $CO_2$ shows miscible characteristics with the $n C_7$ oil phase, which improves the movement ability of alkane molecules and enlarges the oil phase. Therefore, $CO_2$ molecules can strongly promote the movement of $n C_7$ molecules and the development of $n C_7$.

The detected occurrence states of alkanes on the rock surface have confirmed that $n C_{18}$ and $n C_{25}$ alkanes exhibit the characteristics of a single layer of an oil film, and the molecules themselves have weak motion ability. From Figs.

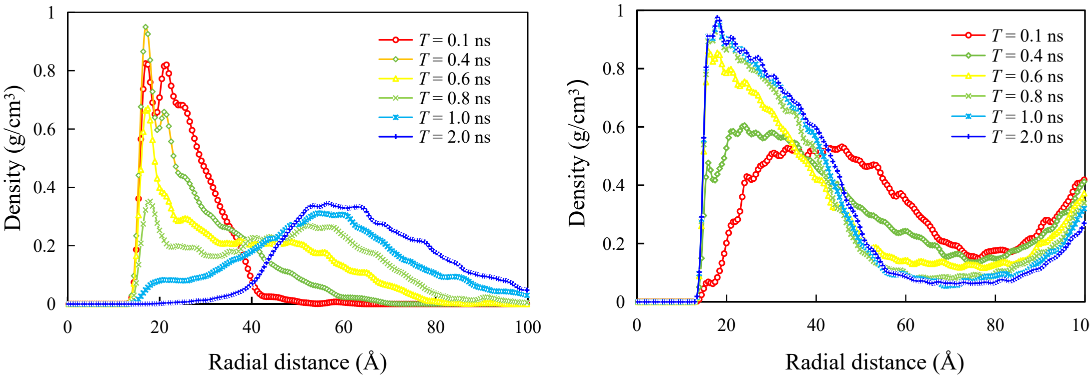

(a) $CO_2$-$nC_7$-$\alpha$-$SiO_2$ system

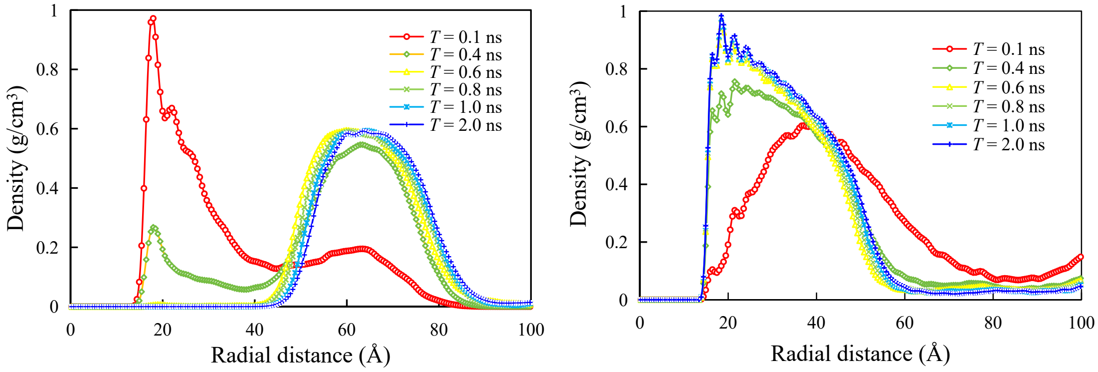

(b) $CO_2$-$nC_{18}$-$\alpha$-$SiO_2$ system

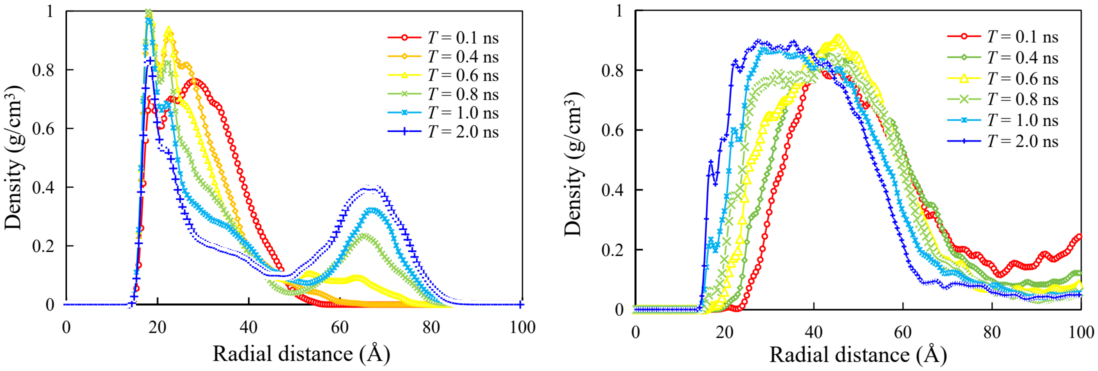

(c) $CO_2$-$nC_{25}$-$\alpha$-$SiO_2$ system

**Fig. 8**. Radial density distribution change of $CO_2$ and alkanes on $\alpha$-$SiO_2$ surface.

7(b) and 7(c), it can be seen that $CO_2$ can also achieve effective stripping of the $nC_{18}$ and $nC_{25}$ systems. With an increase in the chain length of alkane molecules, it is more difficult for $CO_2$ to pass through them (Dong et al., 2023b). This is because the aggregation ability of the alkanes themselves will be strengthened with an increase in the carbon number, resulting in a gradual decrease in the intermolecular gaps between the $nC_{18}$ and $nC_{25}$ systems. Therefore, $CO_2$ will be more prone to strip $nC_{18}$, followed by $nC_{25}$. However, the characteristics displayed are significantly different from those of $nC_7$. After the removal of $nC_{18}$ and heavier alkanes, the oil phase system is more inclined to aggregate into a clump, and no obvious miscibility with $CO_2$ can be observed.

In order to further compare the strip processes and characteristics of $CO_2$ for different alkanes, the $CO_2$ and alkane density distributions are illustrated in Fig. 8. The simulation reveals that the oil film of $nC_7$ alkanes on the rock surface is gradually stripped and destroyed. The peak density of alkanes decreases gradually before 0.4 ns, and the density peak characteristics disappear completely after 0.6 ns. The $nC_7$ system mainly migrates to a radial range of 40~100 Å, and the oil phase distribution range is the largest. Correspondingly, the normal density distribution of $CO_2$ shows a trend opposite to that for $nC_7$. $CO_2$ molecules gradually pass through the $nC_7$ system and contact the rock wall, eventually occupying the entire rock surface and effectively replacing the alkanes.

The density distributions of $nC_{18}$ and $nC_{25}$ show obvious differences from that of $nC_7$. The density peak of $nC_{18}$ disap-

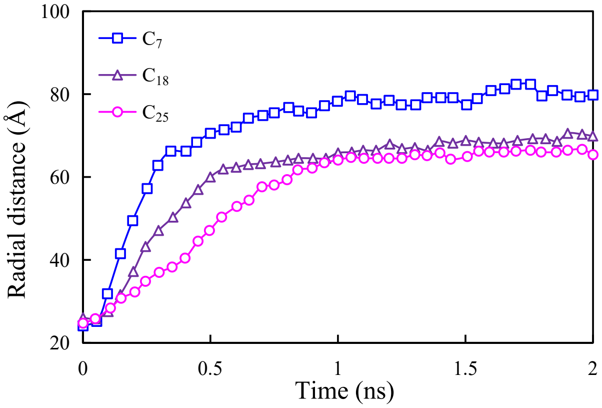

**Fig. 9**. Centroid variation of alkanes in $CO_2$-alkanes-$\alpha$-$SiO_2$ systems.

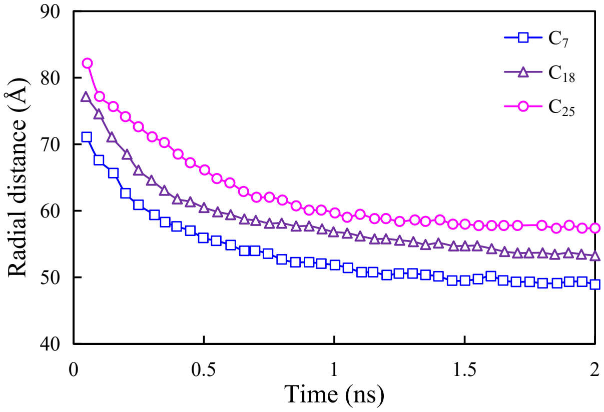

**Fig. 10**. Centroid variation of $CO_2$ in $CO_2$-alkanes-$\alpha$-$SiO_2$ systems.

pears at about 0.4 ns, while that of $nC_{25}$ ceases to be obvious at about 0.8 ns. Meanwhile, the stripped alkane system does not show the good dispersion characteristics of $nC_7$. The densities of $nC_{18}$ and $nC_{25}$ systems after stripping are concentrated in the range of 40∼80 Å, and the alkane system is more inclined to aggregate into a clump, consistent with the distribution characteristics of the oil phase shown in Figs. 7(b) and 7(c). The dispersion ability of the whole alkane system is weak and so as the overall movement ability, which is also the essential reason for the poor fluidity of heavy oil with high molecular weights.

Figs. 9 and 10 present the centroid variations of alkanes and $CO_2$ in different $CO_2$-alkane-$\alpha$-$SiO_2$ systems. The centroid variations of a light alkane change more rapidly than those of a heavy alkane, and the displacement ranges are larger, which further intuitively shows that the replacement effect of $CO_2$ is better for light alkanes than for heavy alkanes (Huang et al., 2024).

## 3.3 MD mechanism analysis of $CO_2$ replacing oil

In order to understand the kinetic mechanisms of $CO_2$ replacing oil molecules from a rock surface, the $nC_7$ system is taken as an example and its replacement process is analyzed in detail. By studying the process of molecular motion and the relative motion trajectories of $CO_2$ and $nC_7$ molecules, the replacement process of the oil film on the surface of $\alpha$-$SiO_2$ can be divided into four typical stages and a supplementary stage, as shown in Fig. 11.

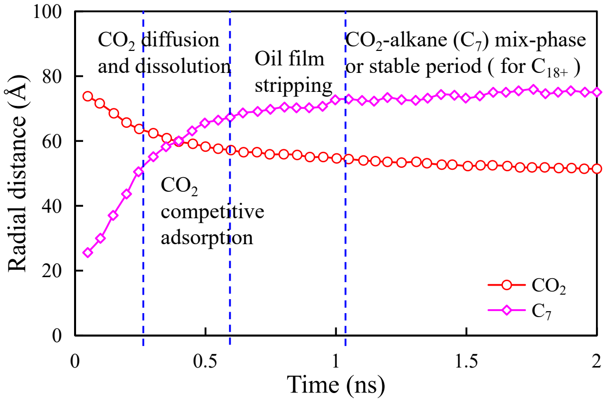

**Fig. 11**. Stage division of $CO_2$ stripping of oil molecules from $\alpha$-$SiO_2$ surface.

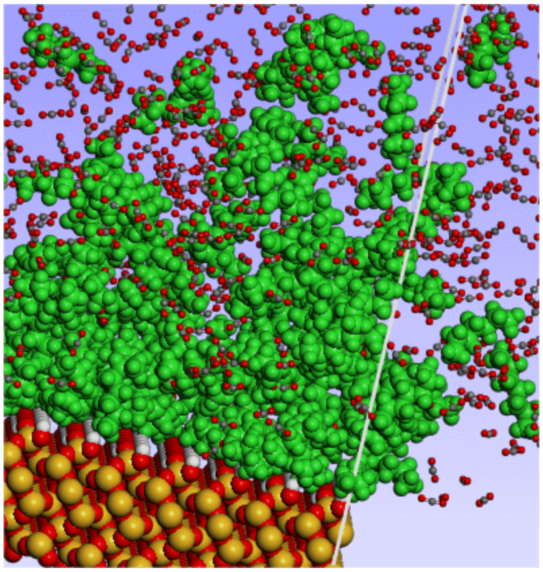

**Fig. 12**. Diffusion movement of $CO_2$ in oil phase (alkane system).

### 3.3.1 $CO_2$ diffusion stage

At this stage, the diffusion and dissolution capacities of $CO_2$ play a dominant role, and the relative displacements of $CO_2$ and alkane molecules are the most drastic changes. In the initial state, $CO_2$ and alkanes occupy their respective phase spaces with obvious phase interfaces. However, as the restriction of molecular movement is lifted and the simulation begins, the contact interface between $CO_2$ and $nC_7$ changes from the original flat to a rough one and the interface is fused together (Fig. 12), which is comparable to the descriptions by Wang et al. (2022b). The outermost alkane molecules stretch first and $CO_2$ can pass through the gaps between alkane molecules depending on its diffusion and dissolution ability in the oil phase. The $CO_2$ content in the oil phase gradually increases and the stretching effect of alkane molecules is

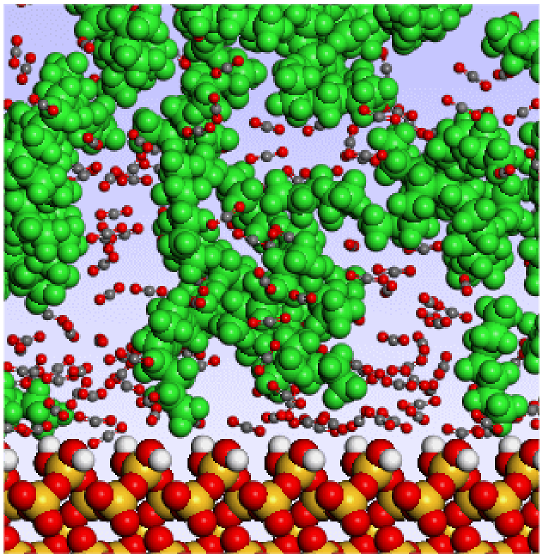

**Fig. 13**. Competitive adsorption effect between $CO_2$ and $nC_7$ on $\alpha$-$SiO_2$ surface.

more significant, which corresponds to the expansion effect of $CO_2$ in the oil phase. From the microscopic perspective, $CO_2$ not only increases the volume of the oil phase but also enlarges the interspace between alkane molecules, forming the advantageous diffusion channels of $CO_2$ (Wang et al., 2022a).

### 3.3.2 Competitive adsorption stage

When $CO_2$ passes through the alkane molecules (oil film), it comes into contact with the innermost $SiO_2$ wall. The mass of $CO_2$ molecules is much smaller than that of the alkane molecules, and it is more significantly affected by the hydroxyl group on the surface of $\alpha$-$SiO_2$. Previous studies have proven that the modified hydrogen bond between $CO_2$ and $\alpha$-$SiO_2$ can promote the adsorption of $CO_2$ molecules on the quartz surface (Qin et al., 2008; Sui et al., 2024), which is in agreement with the simulation illustrated in Fig. 13. $CO_2$ shows a stronger adsorption effect on the rock surface compared with alkane molecules, with the molecular motion process entering the stage of competitive adsorption (Fig. 13). The effect of $SiO_2$ molecules in the innermost layer on alkane molecules is initially strong and binding, and $CO_2$ is dominated by competitive adsorption. Subsequently, the $SiO_2$ adsorption sites formerly occupied by alkane molecules are grabbed away, which causes $CO_2$ to continuously displace the innermost alkane molecules on the surface of $\alpha$-$SiO_2$. Finally, the alkanes are gradually replaced by $CO_2$ on the surface of $\alpha$-$SiO_2$. According to the change of centroid displacement, as shown in Fig. 11, the change trend of $CO_2$ and alkane displacement in this stage is from abrupt to slow. This is because the number of competitive adsorption sites gradually lessens with an increase in the adsorption amount, and the adsorption amount of $CO_2$ on the surface of $\alpha$-$SiO_2$ has a limit.

### 3.3.3 Oil film displacement stage

As presented in Fig. 14, when $CO_2$ successfully enters the inner oil film and occupies the adsorption site on the surface of $\alpha$-$SiO_2$, the binding force on alkane molecules becomes smaller and thus their movement becomes freer. In this process, the alkane molecules will move farther away from the $\alpha$-$SiO_2$ surface and in the opposite direction of $CO_2$. Finally, the alkanes, or oil films, are completely pushed away from the $\alpha$-$SiO_2$ surface by the action of $CO_2$ molecules.

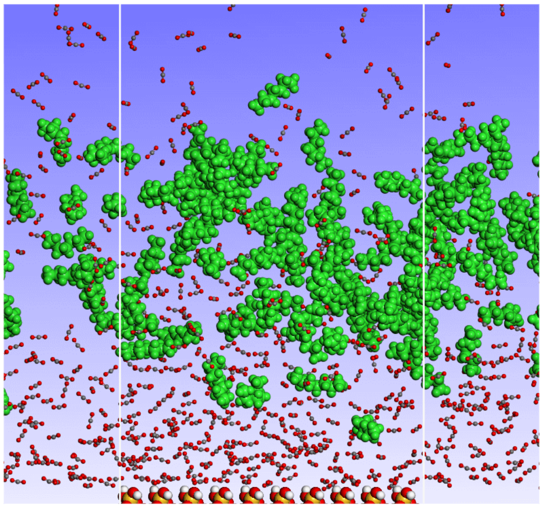

**Fig. 14**. $CO_2$ strips oil film on $\alpha$-$SiO_2$ surface.

### 3.3.4 $CO_2$-alkanes miscible phase

For the $nC_7$ alkane with a low carbon number, there is a fourth phase of movement between $CO_2$ and alkanes, that is, the miscible phase, as shown in Fig. 15(a). Most of the $CO_2$ is mixed with the low-carbon alkane molecules and the interface between the oil phase and the $CO_2$ phase gradually disappears. The mobility of the mixed phase increases and the viscosity of the macroscopic system will be significantly reduced. However, even though heavy alkane molecules can be replaced by $CO_2$ through competitive adsorption, they still remain in clumps or thick layers, which are difficult to mix with $CO_2$ and become more dispersed (Dong et al., 2023b; Huang et al., 2024), as shown in Fig. 15(b).

## 4. Conclusions

In this paper, molecular dynamics simulations are performed to study the occurrence characteristics of different alkanes on a $\alpha$-$SiO_2$ surface, and the process of $CO_2$ replacing crude oil is simulated to explore the EOR mechanisms of $CO_2$ for shale oil from the micro perspective, to provide a theoretical reference for the application of $CO_2$ for enhanced shale oil recovery. Some conclusions can be drawn as follows:

1) Various alkanes occur in the state of a single-layer oil film on the surface of $\alpha$-$SiO_2$. $CO_2$ injection can achieve the effective replacement of different alkanes on the surface of $\alpha$-$SiO_2$, and the stripping time extends with an increase in the carbon number.
2) Through the alkane molecular gaps, $CO_2$ passes through the alkane molecular system and reaches the rock surface to achieve effective stripping of the oil films of different alkane molecules. $CO_2$ is much easier to mix with the stripped oil molecules and displace them from the rock

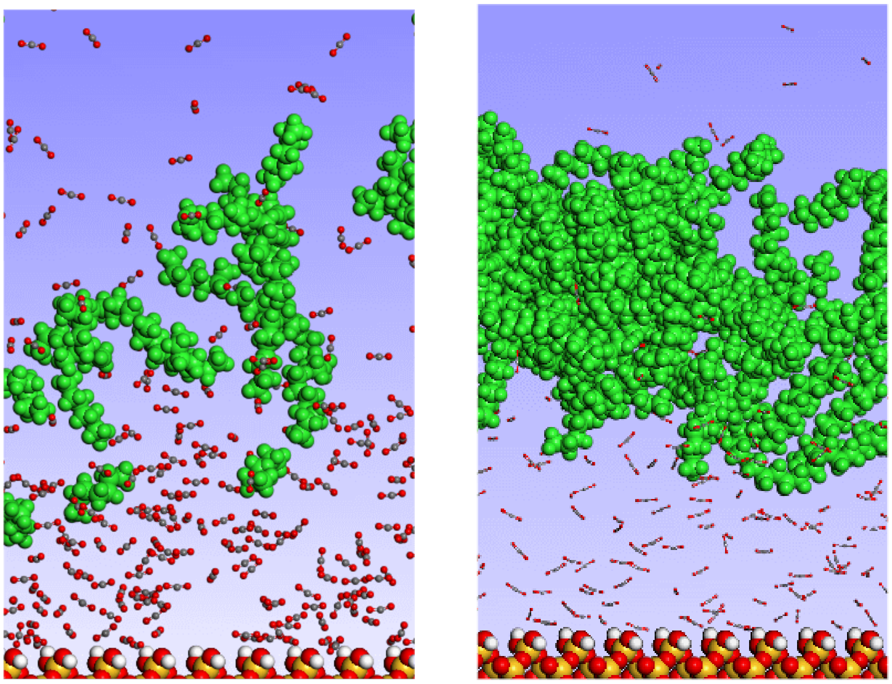
(a) $n\mathrm{C}_7$ (b) $n\mathrm{C}_{25}$

**Fig. 15**. Mixing process of $CO_2$ with stripped alkanes.

surface when the carbon number is small.

3) The process of stripping alkanes on a $\alpha$-$SiO_2$ surface by $CO_2$ can be mainly divided into four stages. First, $CO_2$ mixes with crude oil under diffusion and dissolution mechanisms. Next, the alkane molecules on the surface of $\alpha$-$SiO_2$ are stripped by $CO_2$ under a competitive adsorption mechanism to achieve a substitution of alkane molecules. During the third stage, after $CO_2$ has filled up the space on the rock surface, $CO_2$ is further enriched and thickened on the rock surface and displaces the entire alkane system. For light alkanes, there is a fourth miscible stage, in which $CO_2$ is mixed with alkane molecules to form a homogeneous system to improve the flow capacity of the oil phase. However, once heavy alkanes have been displaced, it is difficult for $CO_2$ to mix with them.

## Acknowledgements

This work was supported by the National Natural Science Foundation of China (No. 42130803), the National Key Basic R&D Program (No. 2022YFF0801200), the State Key Laboratory of Petroleum Resources and Prospecting, China University of Petroleum (No. PRP/open-2216), and the Knowledge Innovation Program of Wuhan-Shuguang.

## Conflict of interest

The authors declare no competing interest.

## References

Alafnan, S. Carbon dioxide and methane sequestration in organic-rich shales: Nanoscale insights into adsorption and transport mechanisms. Journal of Energy Resources Technology, 2022, 144(7): 073010.

Alfarge, D., Wei, M., Bai, B. Factors affecting $CO_2$-EOR in shale-oil reservoirs: Numerical simulation study and pilot tests. Energy & Fuels, 2017, 31(8): 8462-8480.

Cui, F., Jin, X., Liu, H., et al. Molecular modeling on Gulong shale oil and wettability of reservoir matrix. Capillarity, 2022, 5(4): 65-74.

Dong, X., Xu, W., Liu, H., et al. Molecular insight into the oil displacement mechanism of $CO_2$ flooding in the nanopores of shale oil reservoir. Petroleum Science, 2023a, 20: 3516-3529.

Dong, X., Xu, W., Liu, H., et al. On the replacement behavior of $CO_2$ in nanopores of shale oil reservoirs: Insights from wettability tests and molecular dynamics simulations. Geoenergy Science and Engineering, 2023b, 223: 211528.

Fang, T., Zhang, Y., Ma, R., et al. Oil extraction mechanism in $CO_2$ flooding from rough surface: Molecular dynamics simulation. Applied Surface Science, 2019, 494(15): 80-86.

Feng, Q., Xu, S., Xing, X., et al. Advances and challenges in shale oil development: A critical review. Advances in Geo-Energy Research, 2020, 4(4): 406-418.

Gou, Q., Xu, S., Chen, Z. Full-scale pores and micro-fractures characterization using FE-SEM, gas adsorption, nano-CT and micro-CT: A case study of the Silurian Longmaxi

Formation shale in the Fuling area, Sichuan Basin, China. Fuel, 2019, 253(1): 167-179.

Guo, H., Wang, Z., Wang, B., et al. Molecular dynamics simulations of oil recovery from dolomite slit nanopores enhanced by $CO_2$ and $N_2$ injection. Advances in Geo-Energy Research, 2022, 6(4): 306-313.

Huang, T., Cheng, L., Cao, R., et al. Molecular simulation of the dynamic distribution of complex oil components in shale nanopores during $CO_2$-EOR. Chemical Engineering Journal, 2024, 479: 147743.

Jin, L., Hawthorne, S., Sorensen, J., et al. Advancing $CO_2$ enhanced oil recovery and storage in unconventional oil play-experimental studies on Bakken Shales. Applied Energy, 2017, 208: 171-183.

Jin, Z., Firoozabadi, A. Methane and carbon dioxide adsorption in clay-like slit pores by Monte Carlo simulations. Fluid Phase Equilibria, 2013, 360: 456-465.

Liu, B., Wang, C., Zhang, J., et al. Displacement mechanism of oil in shale inorganic nanopores by supercritical carbon dioxide from molecular dynamics simulations. Energy & Fuels, 2017, 31: 738-746.

Michael, G., Vello, K., Phil, D. Opportunities for using anthropogenic $CO_2$ for enhanced oil recovery and $CO_2$ storage. Energy and Fuels, 2013, 27(8): 4183-4189.

Pathak, M., Huang, H., Meakin, P., et al. Molecular investigation of the interactions of carbon dioxide and methane with kerogen: Application in enhanced shale gas recovery. Journal of Natural Gas Science and Engineering, 2018, 51: 1-8.

Qin, Y., Yang, X., Zhu, Y., et al. Molecular dynamics simulation of interaction between supercritical $CO_2$ fluid and modified silica surfaces. Journal of Physical Chemistry C, 2008, 112(33): 12815-12824.

Santos, M., Franco, L., Castier, M., et al. Molecular dynamics simulation of n-alkanes and $CO_2$ confined by calcite nanopores. Energy & Fuels, 2018, 32(2): 1934-1941.

Sheng, J. Critical review of field EOR projects in shale and tight reservoirs. Journal of Petroleum Science and Engineering, 2017, 159: 654-665.

Sui, H., Zhang, F., Zhang L., et al. Competitive sorption of $CO_2/CH_4$ and $CO_2$ capture on modified silica surfaces: A molecular simulation. Science of The Total Environment, 2024, 908: 168356.

Sun, S., Liang, S., Liu, Y., et al. A review on shale oil and gas characteristics and molecular dynamics simulation for the fluid behavior in shale pore. Journal of Molecular Liquids, 2023, 376: 121507.

Wang, H., Su, Y., Wang, W., et al. $CO_2$-oil diffusion, adsorption and miscible flow in nanoporous media from pore-scale perspectives. Chemical Engineering Journal, 2022a, 450: 137957.

Wang, H., Wang, X., Jin, X., et al. Molecular dynamics simulation of diffusion of shale oils in montmorillonite. The Journal of Physical Chemistry C, 2016a, 120(16): 8986-8991.

Wang, R., Bi, S., Guo, Z., et al. Molecular insight into replacement dynamics of $CO_2$ enhanced oil recovery in nanopores. Chemical Engineering Journal, 2022b, 440: 135796.

Wang, S., Feng, Q., Javadpour F., et al. Oil adsorption in shale nanopores and its effect on recoverable oil-in-place. International Journal of Coal Geology, 2015, 147-148: 9-24.

Wang, S., Javadpour, F., Feng, Q. Molecular dynamics simulations of oil transport through inorganic nanopores in shale. Fuel, 2016b, 171: 74-86.

Wang, S., Yao, X., Feng, Q., et al. Molecular insights into carbon dioxide enhanced multi-component shale gas recovery and its sequestration in realistic kerogen. Chemical Engineering Journal, 2021, 425: 130292.

Wan, Y., Jia, C., Lv, W., et al. Recovery mechanisms and formation influencing factors of miscible $CO_2$ huff-n-puff processes in shale oil reservoirs: A systematic review. Advances in Geo-Energy Research, 2024, 11(2): 88-102.

Xue, C., Ji, D., Cheng, D., et al. Adsorption behaviors of different components of shale oil in quartz slits studied by molecular simulation. ACS Omega, 2022, 7(45): 41189-41200.

Yan, Y., Dong, Z., Zhang, Y., et al. $CO_2$ activating hydrocarbon transport across nanopore throat: Insights from molecular dynamics simulation. Physical Chemistry Chemical Physics, 2017, 19(45): 30439-30444.